

CONF-8909275-1

UCRL-102238
PREPRINT

Received by GSI

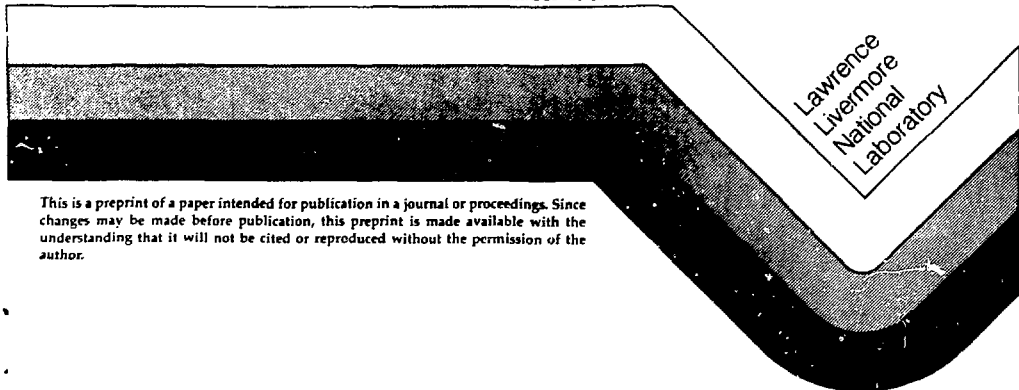
DEC 11 1989

ION-HEATED THERMAL COMPTONIZATION MODELS
AND
X-RAY SPECTRAL CORRELATIONS IN ACTIVE GALACTIC NUCLEI

Charles D. Dermer

This paper was submitted for publication in the
Proceedings of the 23rd ESLAB Symposium on
X-Ray Astronomy Bologna, Italy,
September 13-20, 1989

November 1989



This is a preprint of a paper intended for publication in a journal or proceedings. Since changes may be made before publication, this preprint is made available with the understanding that it will not be cited or reproduced without the permission of the author.

DISTRIBUTION OF THIS DOCUMENT IS UNLIMITED

DISCLAIMER

This document was prepared as an account of work sponsored by an agency of the United States Government. Neither the United States Government nor the University of California nor any of their employees, makes any warranty, express or implied, or assumes any legal liability or responsibility for the accuracy, completeness, or usefulness of any information, apparatus, product, or process disclosed, or represents that its use would not infringe privately owned rights. Reference herein to any specific commercial products, process, or service by trade name, trademark, manufacturer, or otherwise, does not necessarily constitute or imply its endorsement, recommendation, or favoring by the United States Government or the University of California. The views and opinions of authors expressed herein do not necessarily state or reflect those of the United States Government or the University of California, and shall not be used for advertising or product endorsement purposes.

ION-HEATED THERMAL COMPTONIZATION MODELS
AND
X-RAY SPECTRAL CORRELATIONS IN ACTIVE GALACTIC NUCLEI

UCRL--102238

Charles D. Demer

DE90 003597

Physics Department, Lawrence Livermore National Laboratory

P.O. Box 808, L-297, Livermore, CA 94550 USA

ABSTRACT

Recent Ginga observations of the Seyfert 1 galaxies NGC 4051 and MCG 6-30-15 show a positive correlation between the 2-10 keV luminosity and photon spectral index α . Similar behavior has also been reported in Exosat and Einstein observations of other active galactic nuclei, and is suggested in hard X-ray low-state data of the galactic black-hole candidate Cygnus X-1. A two-temperature thermal Comptonization model with internal soft-photon production provides a simple explanation for this correlation. The electron temperature, determined by a balance between ion heating and radiative cooling, decreases in response to an enhancement of the soft photon flux, resulting in a softening of the spectrum and an increase in the soft X-ray luminosity. The bulk of the soft photons are produced through pion production in collisions between the hot ions. Pivoting of the spectrum at photon energies $\epsilon > 50$ keV is a consequence of variations in the ion temperature. An important test of the model would be time correlations between soft and hard X-ray bands.

Keywords: Active galactic nuclei; X-rays: spectra and variability

I. INTRODUCTION

The origin of the variable, luminous X- and γ -radiation emitted by active galactic nuclei (AGN) and other black-hole sources remains a puzzle, although Compton or Compton-synchrotron processes seem to be required in order to satisfy luminosity and time-variability constraints. Any convincing model for the high-energy emission of AGN must, however, be able to explain a number of observational features, including the tight clustering of the 2-10 keV X-ray photon spectral index near $\alpha \approx 0.7$ (Ref. 1), and spectral softening at γ -ray energies, which is required in order not to conflict with the measured intensity of the extragalactic γ -ray background radiation (Ref. 2). Furthermore, values of the 2-10 keV X-ray compactness parameter $l_{2,10}$, deduced from X-ray variability time scales, are observed to fall in the range $\sim 0.05 - 10$ (Ref. 3). In recent years, evidence has also been accumulating for another important observational characteristic of the high-energy emission from AGN. This is the appearance of a positive correlation between the soft X-ray intensity and spectral softness. This correlation has been reported in five Seyfert 1 galaxies (Refs. 4,5,6,7), and is inferred from Exosat data of a narrow emission line galaxy (Ref. 8). Notably, it was not seen in Exosat observations (Ref. 9) of a Seyfert 2 galaxy. This behavior is also apparent in hard X-ray data of Cygnus X-1, suggesting an underlying connection between the radiation mechanisms operating in solar mass and supermassive black-hole sources.

Here, results of a two-temperature thermal model (Ref. 10) are used to explain the correlation between spectral index and luminosity seen in the high-energy emission from black-hole sources. This model was proposed last year to account for the

range of values of α and $l_{2,10}$ observed in AGN. The model depends on only two parameters: the Thomson depth τ_T of the system, and the ion temperature T_i . The correlation between X-ray spectral index and intensity is interpreted as being due to changes in the ion temperature, with τ_T remaining constant. A good fit to measurements of α as a function of X-ray intensity for a number of AGN is obtained. A number of clearcut predictions follow from this model. Most important is the appearance of a softening in the spectrum at $\epsilon \sim$ several hundred keV, corresponding to the thermal turnover in the electron distribution. A high energy tail at MeV energies, associated with pion processes, is also expected. Also, hard X-rays variations should lag behind variations in the soft X-ray flux because thermal Comptonization of soft photons from soft to hard energies is responsible for the formation of the X-ray spectrum. Observations of these signatures would provide strong evidence for the validity of this model.

II. HOT ION MODEL

We make use of model results published in Ref. 10, without further modification. The premise of the model is that the high-energy radiation emitted from the central engine of AGN initially resides in thermal ions with temperatures T_i between ~ 10 and 200 MeV. If a significant fraction of the ions' thermal energy is converted into radiation, ion temperatures in this range are in accord with estimates that $\sim 10\%$ of the rest-mass energy of the accreting matter is converted into radiant energy. Radiation from pion production alone is too inefficient to provide this luminosity, since $\sim 70\%$ of the mass energy in pions is converted into neutrinos. If an electron plasma is present, as required by charge neutrality, Coulomb losses from the ions to the electrons can be much more important than energy losses through pion production provided that the electron plasma temperature $T_e < 0.5$ MeV (Fig. 7, Ref. 11). If the value of T_e is governed by the condition of thermal balance, electron temperatures below ~ 1 MeV are expected from the weakness of Coulomb coupling between ions and electrons. Collective processes could transfer ion kinetic energy to the thermal electrons more rapidly than is possible through Coulomb coupling. But pair production becomes important when the electron temperature exceeds ~ 1 MeV, so that again, electron temperatures in excess of ~ 1 MeV are not expected. For simplicity, collective processes are assumed not to be important here.

The electrons in the thermal plasma can efficiently radiate their energy through thermal bremsstrahlung, thermal cyclotron-synchrotron emission, and through thermal Comptonization of soft photons. Cyclotron and synchrotron emission are, of course, only important when a magnetic field is present. The magnetic field strength in an accretion plasma is unfortunately very uncertain. In this model, an equipartition magnetic field is assumed.

DISTRIBUTION OF THIS DOCUMENT IS UNLIMITED

MASTER

Soft photons are generated not only through bremsstrahlung and thermal cyclo-synchrotron emission, but also through synchrotron emission of pion-decay electrons and positrons formed in collisions of the hot ions. In fact, Comptonization of synchrotron photons radiated by pion-decay positrons becomes the most important cooling mechanism of the thermal electrons when $T_i > 20$ MeV. It may be surprising that pion production is so important, since the average ion energy in the distribution is well below the threshold value for pion production (~ 300 MeV kinetic energy for a proton). But the center-of-mass energy can often exceed the pion production threshold energy in collisions between ions in a self-interacting distribution, since in this case both particles are energetic.

Model results (Ref. 10) giving α as a function of l_{2-10} are shown in Fig. 1. Also shown are compiled data (Ref. 3). If L_{2-10} is the luminosity in the 2-10 keV X-ray band and R is the radius of the emission region, assumed to be spherical, the 2-10 keV X-ray compactness is defined by the relation

$$l_{2-10} = \frac{L_{2-10} [\text{erg s}^{-1}] / R[\text{cm}]}{(m_e c^3 / \sigma_T)} \quad (1)$$

where $m_e c^3 / \sigma_T = 3.7 \times 10^{28}$ erg $\text{s}^{-1} \text{cm}^{-1}$. Lightman and Zdziarski (Ref. 3) obtain values of l_{2-10} for specific AGN by relating R to the X-ray variability time scale Δt_x through the expression $R = c \Delta t_x$. This gives a lower limit to the compactness of the source since R could be smaller than the size inferred from the variability time scale. Arguments (Ref. 12) have, however, been advanced that it is incorrect to infer the source size from an e-folding, or doubling, time scale, because of the $1/f$ character of the X-ray emission. According to this reasoning, if one waits long enough, the preferred criterion for variability will ultimately be met. In the results presented below, we follow the conventional interpretation that the minimum variability time scale gives a measure of the source size. Better agreement with the data can be obtained if this identification is not followed.

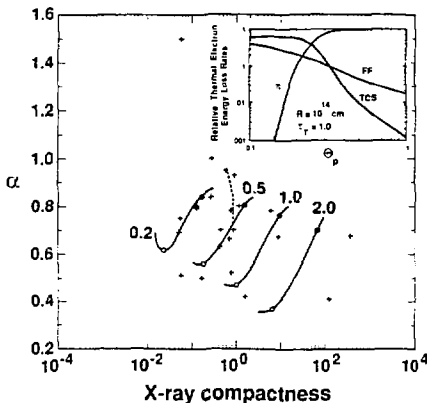


Fig. 1. Model results (Ref. 10) giving the X-ray spectral index α as a function of the X-ray compactness l_{2-10} defined in equation (1). Solid curves are labeled by the Thomson depth τ_T , and map the variation in the α - l_{2-10} dependence when the ion temperature T_i varies between ~ 10 and 200 MeV. The open and filled circles mark $T_i = 20$ and 200 MeV, respectively. The crosses are the compiled data (Ref. 3). The inset shows relative thermal electron energy loss rates through bremsstrahlung (FF), thermal cyclo-synchrotron emission (TCS), and thermal Comptonization of synchrotron soft-photons radiated by pion-decay electrons and positrons (π). Here, $\Theta_p = T_i / 938$ MeV.

The range of calculated compactnesses shown in Fig. 1 generally agrees with observed values of l_{2-10} . Values of α calculated from the hot ion model lie in the range ~ 0.4 - 0.9 , and are also in general agreement with observed values. Values of $\alpha = 0.7$ are associated with $T_i \sim 50$ MeV, depending precisely on the value of τ_T . In some cases, spectral indices greater than unity are observed. This may indicate that the equipartition assumption for the magnetic field is wrong, or that an additional soft photon sources exists. One such source may be related to the soft X-ray excess observed in many AGN. The origin of this excess could be from an optically thick accretion disk located far from the central source.

Fig. 1 also shows that if τ_T is held constant, the X-ray spectrum softens as the ion temperature increases. A clearer understanding of this behavior can be obtained from Fig. 2, where X-ray and soft γ -ray spectra are plotted for a number of values of T_i (the hard MeV signature of pion radiation is not shown here). Note the exponential cutoff in the spectra, and the pivoting of the spectra around values of a few hundred keV with changes in T_i .

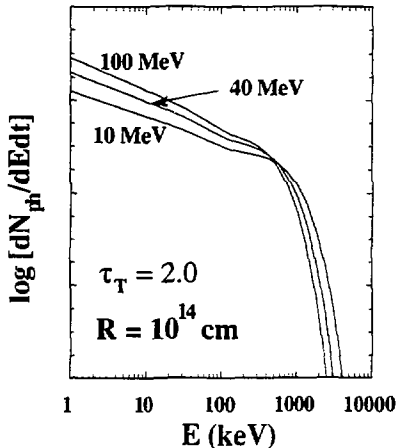


Fig. 2. Thermal Comptonization spectra are shown for $\tau_T = 2$, $R = 10^{14}$ cm, and $T_i = 10, 40$ and 100 MeV. The hard γ -ray signature from pion processes is not shown. Synchrotron radiation from pion-decay electrons and positrons produce most of the soft photons when $T_i > 20$ MeV. The 2-10 keV X-ray spectral index α is equal to $0.36, 0.55$, and 0.72 for $T_i = 10, 40$ and 100 MeV, respectively.

III. OBSERVATIONS AND MODEL RESULTS

Using equation (1), we find that the X-ray compactness in a given waveband is related to the measured energy flux and variability time scale through the expression

$$l_x = \frac{4\pi z^2 \sigma_T F_x}{m_e c^2 H_0^2 \Delta t} = \frac{3.9 z^2 F_{x,11}}{h_0^2 \Delta t_3} = \frac{K F_{x,11}}{h_0^2 \Delta t_3} \quad (2)$$

Here, $cz = 0.01cz_2$ is the recession velocity of the galaxy, $H_0 = 50 h_0 \text{ km s}^{-1} \text{ Mpc}^{-1}$ is Hubble's constant ($1 \leq h_0 \leq 2$), we use $h_0 = 1$ throughout, $\Delta t = 10^3 \Delta t_3$ seconds is the minimum X-ray variability time scale, and $F_x = 10^{-11} F_{x,11} \text{ erg s}^{-1} \text{cm}^{-2}$ is the energy flux in the X-ray waveband under consideration.

We now compare model results with AGN for which evidence of X-ray spectral correlations are available. Quantities needed to

Table 1: Quantities associated with X-ray observations and modeling of selected active galactic nuclei.

Source	Ref.	z_2	X-Ray Band (keV)	F_{-11} (10^{-11} erg s^{-1} cm^{-2})	K	Δt_3
MCG-6-30-15	4	0.78	2-10	-3-7	2.4	-0.2
NGC .051	4	0.233	2-10	-0.8 - 3.5	0.21	-0.2
Mrk 509	5	3.55	3-10	-4 - 5	49	-10
NGC 5506	9	0.60*	2-6	-3.5 - 7	1.4	-3
3C 120	6	3.3	5.6	-0.2 - 0.6†	42.	-100
NGC 4151	7	0.33	2-10	-10 - 40	0.42	-30

* Ref. 13

† Units of 10^{-11} erg s^{-1} cm^{-2} keV $^{-1}$

evaluate eq. (2) for specific sources are given in Table 1. If the X-ray variability time scale implies a maximum source size R , the compactness is greater than some minimum value computed from equation (2). A range of values of τ_T are therefore not allowed when fitting data, since sources that are too optically thin cannot be sufficiently compact to simultaneously agree with variability and luminosity measurements. One can verify from equation (2) and the values in Table 1 that the model does not violate this restriction.

MCG-6-30-15 is a moderate luminosity Sy 1 galaxy with $L_{2-10} \sim 10^{43}$ erg s^{-1} . This source has been observed with both Exosat (Ref. 14) and Ginga (Ref. 4). Deconvolution of the X-ray spectra requires a model for X-ray absorption by surrounding material. The favored model in the Ginga analysis is a partial (~60%) covering model with $N_{\text{H}} = 6(+4, -2) \times 10^{24}$ cm^2 , including emission from cold Fe. The deconvolved data, shown in Fig. 3, strongly indicate a positive correlation between α and L_{2-10} . Also shown are model results with $\tau_T = 2.0$. A good fit to the data is obtained at low luminosities, but the model spectra are somewhat harder than observations at higher luminosities.

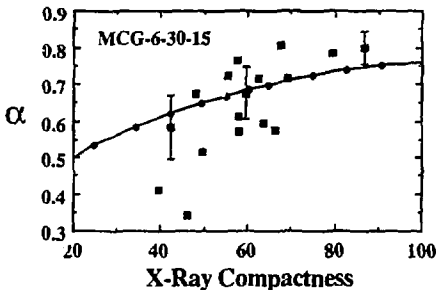


Fig. 3. The data points show results of an analysis of 2-10 keV X-ray data of MCG-6-30-15 (Ref. 4). The inferred compactnesses correspond to $\Delta t_3 = 0.2$. Solid curve shows model results with $\tau_T = 2.0$.

NGC 4051 is a Sy 1 galaxy with $L_{2-10} \sim 4 \times 10^{41}$ erg s^{-1} . Analysis of softness-ratio data from Exosat (Ref. 15) indicates a positive correlation between α and the 2-6 keV X-ray luminosity, which was confirmed by the Ginga results (Ref. 4). The favored model in the Ginga analysis is, again, a partial (~64%) covering model with solar abundances, and a hydrogen column density of $N_{\text{H}} = 14(+4, -2) \times 10^{22}$ cm^2 . Results of the analysis are shown in Fig. 4 along with the model results, with $\tau_T = 0.7$. Again we see general agreement at low luminosities. At high luminosities, again, the model results are slightly harder than the observations.

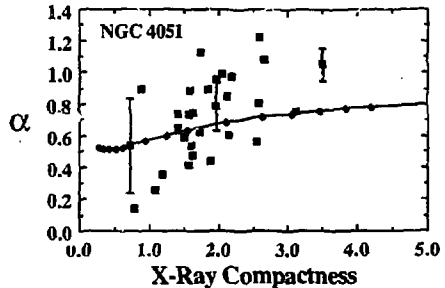


Fig. 4. The data points show results of an analysis of 2-10 keV X-ray data of NGC 4051 (Ref. 4). The inferred compactnesses correspond to $\Delta t_3 = 0.2$. Solid curve shows model results with $\tau_T = 0.7$.

Mrk 509 is a nearby Sy 1 galaxy with $L_{3-10} \sim 2 \times 10^{44}$ erg s^{-1} . Results of an analysis (Ref. 5) of Exosat and Ginga data are shown in Fig. 5. Galactic absorption using galactic abundances with $N_{\text{H}} \approx 4 \times 10^{20}$ cm^2 was used to deconvolve the data. Model spectra with $\tau_T = 2.0$ give a good fit to the data.

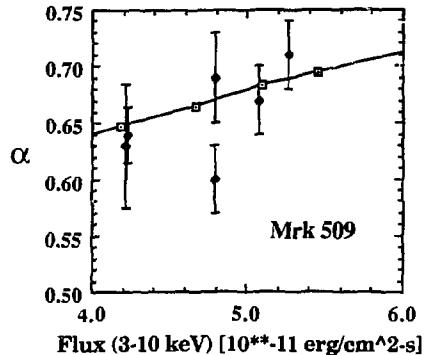


Fig. 5. The data points show results of an analysis of 3-10 keV X-ray Exosat and Ginga data of Mrk 509 (Ref. 5). Solid curve shows model results with $\tau_T = 2.0$.

NGC 5506 is a moderate luminosity Sy 2 galaxy with $L_{2-6} \approx 7 \times 10^{42}$ erg s^{-1} . A uniform cold absorber model with $N_H \approx 2.8 \times 10^{22}$ cm^{-2} was used to determine the X-ray spectrum observed with Exosat (Ref. 9). No evidence for variations of α with luminosity was found, and the best fit value of spectral index was $\alpha = 0.84(\pm 0.04)$. A model fit with $\tau_T = 0.5$ gives a reasonable fit to the data, as shown in Fig. 6. The weak variation of spectral index with luminosity occurs on the high ion-temperature part of the $\tau_T = 0.5$ curve (cf. Fig. 1).

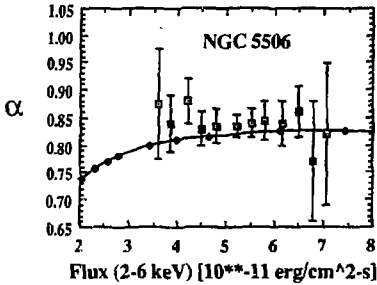


Fig. 6. The data points show results of an analysis of 2-6 keV Exosat data of NGC 5506 (Ref. 9). Solid curve shows model results with $\tau_T = 0.5$.

3C 120 is a Sy 1 galaxy with a compact radio core. Its 2-10 keV luminosity $\approx 1.6 \times 10^{44}$ erg s^{-1} . A uniform cold absorber model with galactic absorption column density $N_H \approx 3 \times 10^{21}$ cm^{-2} was the favored model (Ref. 6). A positive correlation between α and 5.6 keV flux was found, as shown in Fig. 7. As can be seen, the model gives good agreement with the data when $\tau_T = 1.0$.

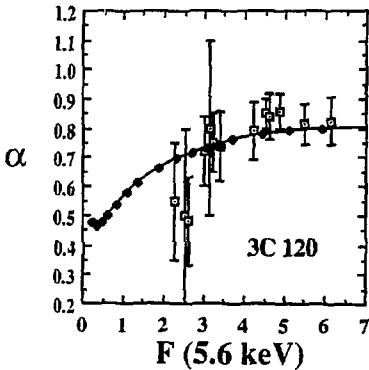


Fig. 7. The data points show results of an analysis of 2-10 keV X-ray Einstein data of 3C 120 (Ref. 6). Solid curve shows model results with $\tau_T = 1.0$.

NGC 4151 is a Sy 1-1.5 with $L_{2-10} \approx 7 \times 10^{42}$ erg s^{-1} . Analysis (Ref. 7) of Exosat observations using a uniform cold absorber model with $N_H \approx 5 \times 10^{22}$ cm^{-2} and an enhanced iron abundance showed a positive correlation of α and F_{2-10} , as shown in Fig. 8. Model results with $\tau_T = 2.0$ give a reasonable fit to the data.

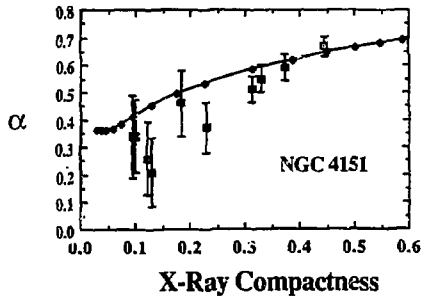


Fig. 8. The data points show results of an analysis of 2-10 keV X-ray Exosat data of NGC 4151 (Ref. 7). Solid curve shows model results with $\tau_T = 2.0$.

X-ray Spectral Correlations in Other Black-Hole Sources: A softness-ratio analysis (Ref. 8) of Exosat data of the narrow emission line galaxy NGC 7314 also suggests a positive correlation between softness ratio and L_{2-10} . It is unfortunately difficult to compare directly with the model because the data are not presented in terms of spectral index variations. Cygnus X-1 also gives some indication for X-ray spectral correlations. In Fig. 9, we have plotted the spectral index as a function of 10-200 keV luminosity using the compilation of Liang and Nolan (Ref. 16). Only low-state data were used. The best fit line through the data show a behavior in accord with observations of spectral correlations in Seyfert 1 galaxies. A more detailed analysis of Cyg X-1 data is, however, required before quantitative model comparisons can be made, since different instruments were used to obtain these data, and the 10-200 keV luminosities were sometimes deduced from extrapolations.

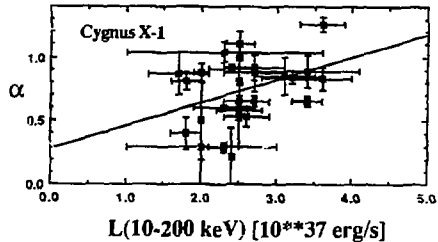


Fig. 9. The data points are values of the hard X-ray spectral index of Cygnus X-1 as a function of 10-200 keV luminosity (from Ref. 16). Also shown is the best fit line given by $\alpha = 0.27 + 0.18 L_{37}$, where L_{37} is the 10-200 keV luminosity in units of 10^{37} erg s^{-1} (all data points were given equal weight).

IV. DISCUSSION AND SUMMARY

The Ginga mission has provided the most convincing evidence yet that the X-ray spectra of Sy 1 galaxies soften as their X-ray luminosities increase. Several examples have been presented in this paper. This behavior is also indicated in low-state hard X-ray data of the galactic black-hole source Cygnus X-1. However, the Sy 2 galaxy NGC 5506 does not show this effect, but the measurement errors are large. An important future study will be to determine whether Sy 1 and Sy 2 galaxies are distinguished by different X-ray spectral index/intensity correlations.

V. REFERENCES

These observations provide an important test for theoretical models of the continuum emission of black-hole sources. As noted in Ref. 9, constant seed thermal Comptonization models with impulsive heating are not in agreement with the data. Pair cascade models, such as those proposed in Ref. 17, may explain this behavior, but these models already have difficulty in obtaining agreement between the X-ray spectral index and MeV cutoff (Ref. 3).

As we have seen, an explanation for the observed spectral correlations is provided by a simple two-temperature hot ion model (Ref. 10). As the ion temperature increases, the injection rate of soft photons emitted by pion-decay positrons and electrons also increases. Thus the spectrum softens and the intensity increases, as shown in Fig. 2. This simple two-parameter model gives reasonable quantitative agreement with the data. Where the model differs from the data, it usually predicts harder spectra than are observed. This may imply that the equipartition assumption for the magnetic field strength is incorrect, or that there is another source of soft photons. Additionally, the dependence of the spectral index on luminosity is not as strong in the model as in the data. This difference may be related to the assumption that the Thomson depth is independent of ion temperature. If a change in the ion temperature were due, for example, to a change in the accretion rate, it is very possible that the Thomson depth would vary due to changes in either the mean ion density or source size of the two-temperature plasma.

This model predicts a thermal cutoff in the spectrum at a few hundred keV and a hard tail from pion production at MeV energies. The spectrum is also expected to pivot at hard X-ray/soft γ -ray energies in response to changes in the ion temperature. Also, hard X-rays are expected to lag soft X-rays. Confirmation of these predictions would strongly suggest the existence of an ion-heated two-temperature plasma in the central engine of black-hole sources.

This work was performed under the auspices of the U. S. Department of Energy by the Lawrence Livermore National Laboratory under contract W-7405-ENG-48.

1. Mushotzky, R.F., 1988, in *Active Galactic Nuclei*, H.R. Miller and P.J. Wiita, eds. (Springer-Verlag: New York), p. 239.
2. Bassani, L., and Dean, A.J., 1983, *Space Sci. Rev.*, **35**, 367.
3. Lightman, A.P., and Zdziarski, A.A., 1987, *Ap. J.*, **319**, 643.
4. Matsuoka, M., Yamauchi, M., Piro, L., and Murakami, T., 1989, *Ap. J.*, submitted.
5. Singh, K.P., Westergaard, N.J., Schnopper, H.W., Awaki, H., and Tawara, Y., these proceedings.
6. Halpern, J.P., *Ap. J.*, **290**, 130.
7. Perola, G.C. et al., 1986, *Ap. J.*, **306**, 508.
8. Turner, T.J., 1987, *M.N.R.A.S.*, **226**, 9p.
9. McHardy, I., and Czerny, B., 1987, *Nature*, **325**, 696.
10. Dermer, C.D., 1988, *Ap. J. (Letters)*, **335**, L5.
11. Dermer, C.D., Liang, E.P., and Canfield, E., 1989, *Ap. J.*, submitted.
12. Lawrence, A., Watson, M.G., Pounds, K.A., and Elvis, M., 1987, *Nature*, **325**, 694.
13. Rubin, V.C., 1978, *Ap. J. (Letters)*, **224**, L55.
14. Pounds, K.A., Turner, T.J., and Warwick, R.S., 1986, *M.N.R.A.S.*, **221**, 7p.
15. Lawrence, A., Watson, M.G., Pounds, K.A., and Elvis, M., 1985, *M.N.R.A.S.*, **217**, 685.
16. Liang, E.P., and Nolan, P.L., 1984, *Space Sci. Rev.*, **38**, 353.
17. Kazanas, D., 1984, *Ap. J.*, **287**, 112.